

LYRA Responsivity: Update

IED 15 Jan 2008 (revised 05 Feb 2008)

Purpose and Contents

This report consists of earlier reports' updates (Sections I and II) and of new simulations (III). The aim is to suggest twelve tables with new values for the LYRA channels' responsivities in the resulting section (IV). These new values should be presented to the concerned team members, checked by them, and agreed on. Consequently, the radiometric model will then be re-calculated, new purities will be figured out, and the calibration software will be re-written accordingly. Together with the fact that, meanwhile, there are four more TIMED/SEE samples available (two pre- and two postflare spectra), this will considerably improve the existing first software approach (see *IED_20061025_LYRA_Calibration.pdf*).

I. BESSY NI March 2007 Measurements page 2 – 5

This is the former report *IED_20071003_LYRA_Respons.pdf*.

II. Consequences of Detector Locations and Flatfields page 6 – 17

This is an updated version of the former report *IED_20070320_LYRA_Detectors.pdf*, revised 21 Nov 2007, with new found coordinates (formerly 0) from GI 2006, and new measurements from NI 2007.

III. Simulations with Davos Solar Spectrum page 18 – 19

This was done in order to correct the long-wavelength extension of the responsivity curves.

IV. Suggested Responsivity Changes page 20 – 23

This section includes information where to download tables for the twelve new responsivity curves, as well as PDFs of other reports.

Appendix page 24 – 26

This includes an example of the above-mentioned tables.

To get a basis for a decision about LYRA responsivities, please read at least pages 2, 10, 18, and 20.

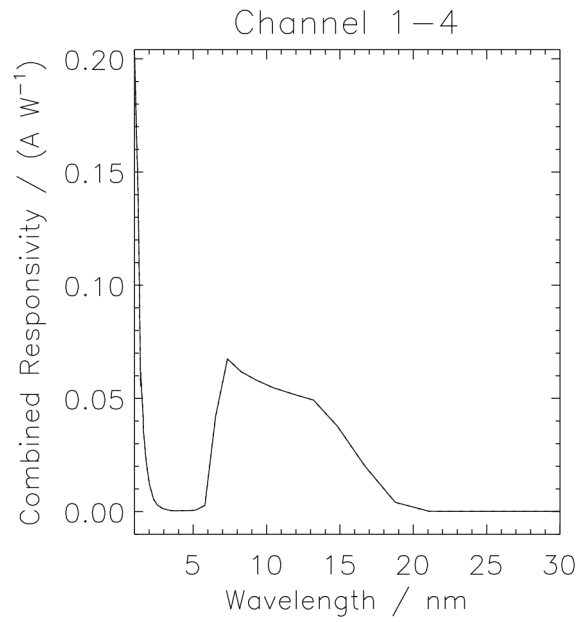
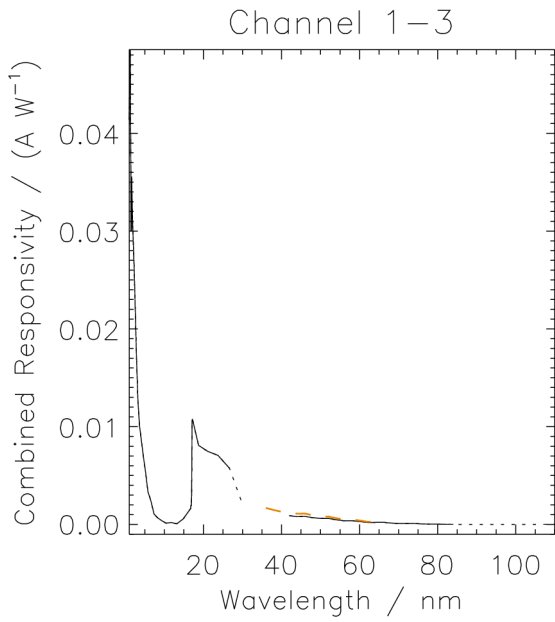
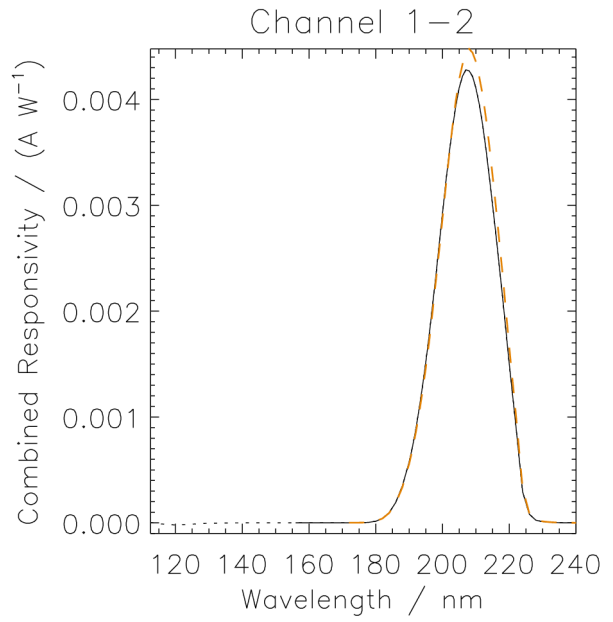
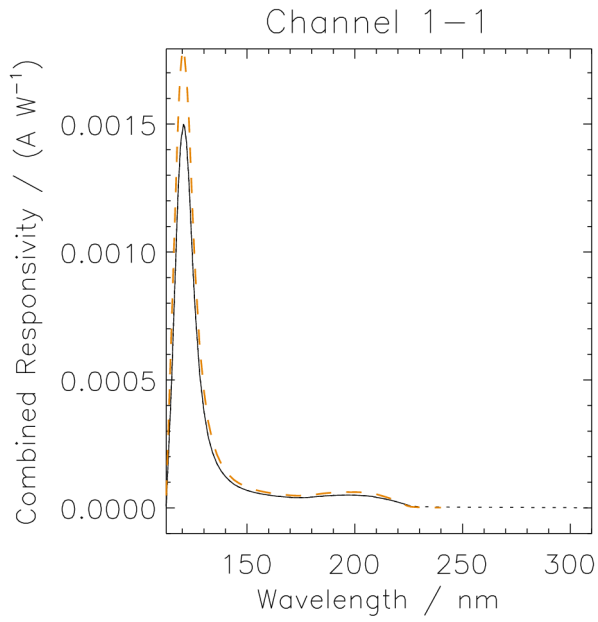
I. BESSY NI March 2007 Measurements

The following table shows the wavelength intervals (in *nm*) for various channels and tests (first column): The BESSY NI and GI campaigns of March 2006 (second column; dotted black lines in the figures below) have led to the selection of intervals for the radiometric model (third column; straight black lines in figures). The BESSY NI campaign of February 2007 (fourth column; red dashed lines in figures) now calls for some new decisions.

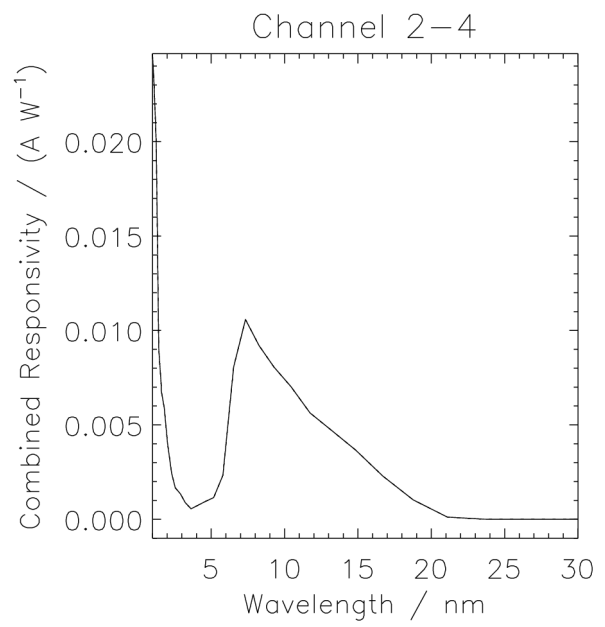
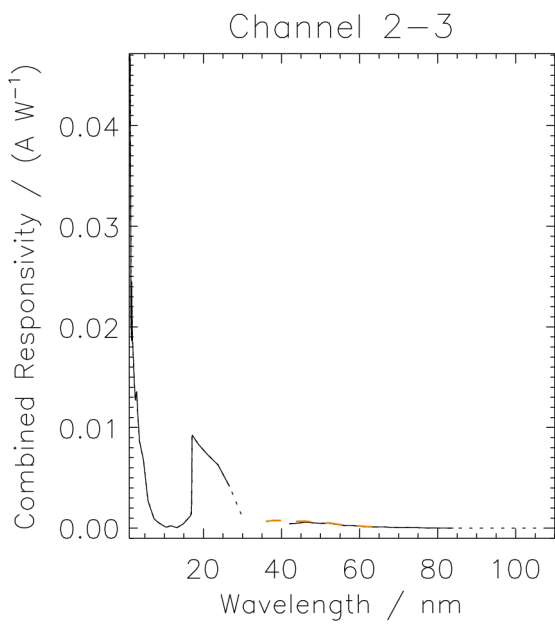
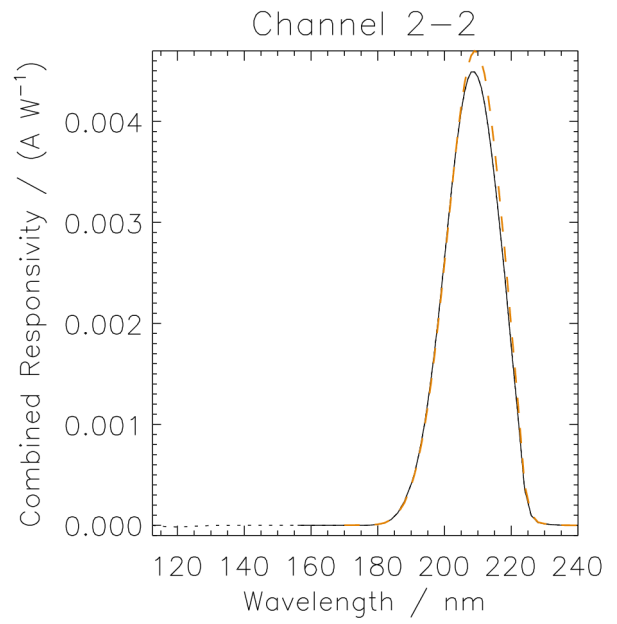
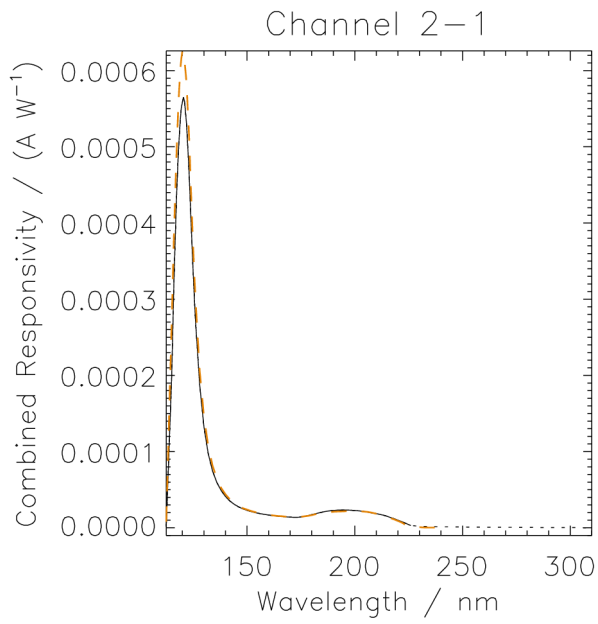
channel	measured 2006	selected 2006	measured 2007	selected 2007
1-1 NI	112.5-310.0	112.5-226.0	112.5-240.0	112.5-240.0
1-2 NI	112.5-240.0	156.0-240.0	172.0-240.0	172.0-240.0
1-3 GI	1.0- 30.0	1.0- 26.7		1.0- 26.7--
1-3 NI	42.0-110.0	42.0- 84.0	36.0- 64.0	--36.0- 84.0
1-4 GI	1.0- 30.0	1.0- 30.0		1.0- 21.1
2-1 NI	112.5-310.0	112.5-226.0	112.5-240.0	112.5-240.0
2-2 NI	112.5-240.0	156.0-240.0	170.0-240.0	170.0-240.0
2-3 GI	1.0- 30.0	1.0- 26.7		1.0- 26.7--
2-3 NI	42.0-110.0	42.0- 84.0	36.0- 64.0	--36.0- 84.0
2-4 GI	1.0- 30.0	1.0- 30.0		1.0- 23.7
3-1 NI	112.5-310.0	112.5-286.0	112.5-240.0	112.5-240.0
3-2 NI	112.5-240.0	156.0-240.0	170.0-240.0	170.0-240.0
3-3 GI	1.0- 30.0	1.0- 26.7		1.0- 26.7--
3-3 NI	42.0-110.0	42.0- 84.0	36.0- 64.0	--36.0- 84.0
3-4 GI	1.0- 30.0	1.0- 30.0		1.0- 21.1

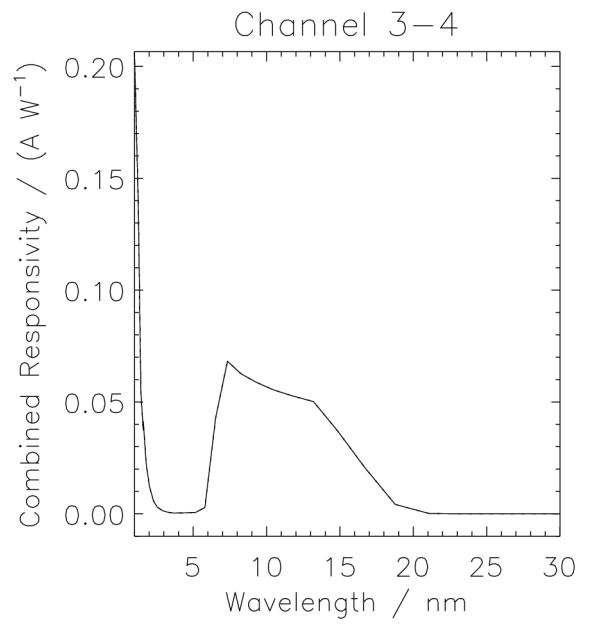
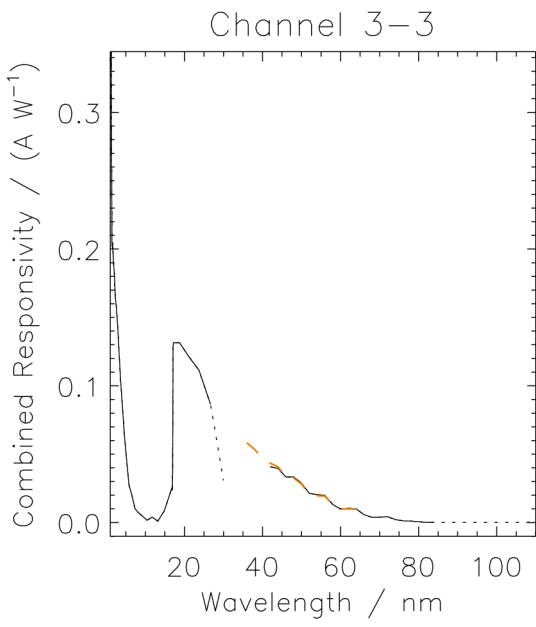
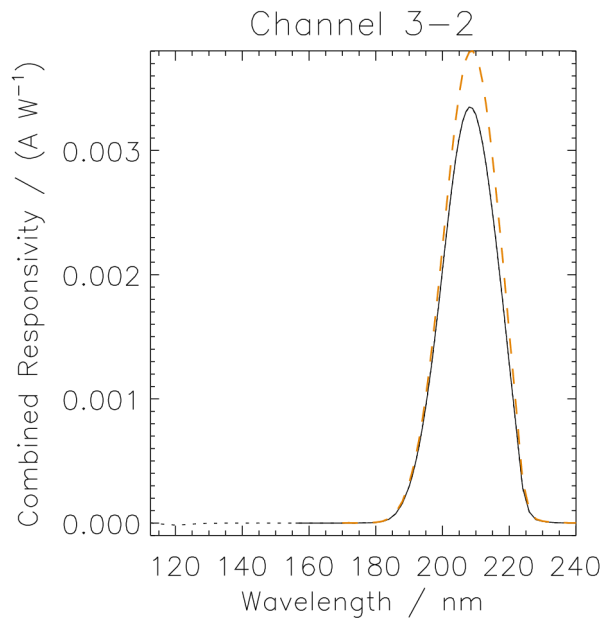
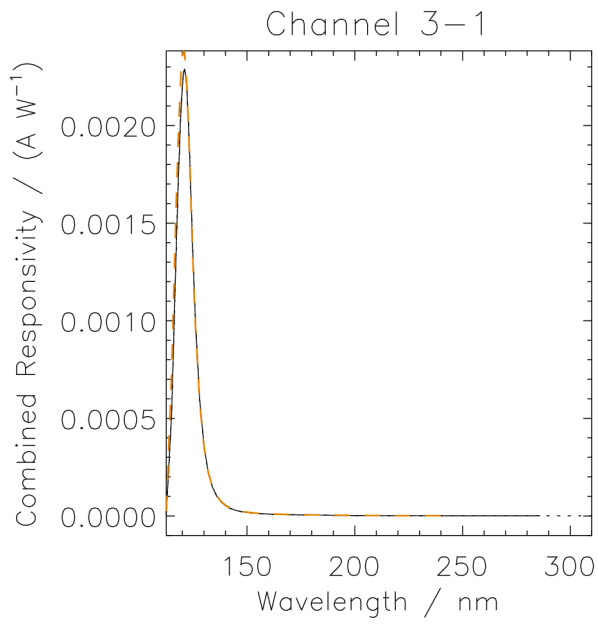
A decision had to be made as of which responsivity measurements should be selected for the radiometric model and its future simulations. Based on earlier decisions as well as considerations about significance and uncertainty, it is suggested to choose the values in the fifth column (above). This includes:

- (1) Cutting the Lyman channel intervals above 240 nm, instead of 226 or 286 nm.
- (2) Cutting the Herzberg channel intervals below ~170 nm instead of 156 nm (several 2006 responsivity measurements below 156 nm were negative).
- (3) Cutting the GI parts of the Aluminium channel intervals at 26.7 nm, i.e. discarding the 30 nm measurements as unreliable.
- (4) Assuming the new (2007 NI campaign) Aluminium channel measurements at 36, 38, and 40 nm as reliable.
- (5) Assuming also to consider the additional “fine resolution” data set for Aluminium channel 2-3 (2007 NI campaign) by averaging the two measurements.
- (6) Assuming a linear interpolation instead of a step function between 26.7 and 36 nm (limits of the GI and NI campaign for the Aluminium channels).
- (7) Cutting the NI part of the Aluminium channel intervals at 84 nm, filling up the interval between 64 and 84 nm with measurements from 2006.
- (8) Averaging the double measurements at 1.42 and 1.60 nm (2006 GI campaign, for Aluminium and Zirconium channel).
- (9) Leaving the Zirconium channel intervals otherwise as they were, between 1 and ~21 nm (several responsivity measurements between ~21 and 30 nm are zero).
- (10) Additionally, as an option, extend the interval into the near UV, visible, and IR spectrum, i.e. up to 1100 or 1240 nm, with the help of the separate filter and detector measurements used for the first radiometric model.



Please **note** that the images on these pages show responsivities according to their last available BESSY campaign, respectively. The complete responsivity curves after the changes suggested according to Sections II and III are shown in section IV (p. 21ff) on a logarithmic scale.





II. Consequences of Detector Locations and Flatfields

The LYRA team collected five sets of detector flatfield measurements, performed in five BESSY campaigns:

- “crosses” from NI 2005 for channels *-1, *-2, *-3
- “crosses” from GI 2005 for channels *-3, *-4
- “surfaces” from NI 2006 for channels *-1, *-2, *-3
- “surfaces” from GI 2006 for channels *-3, *-4
- “surfaces” from NI 2007 for channels *-1, *-2, *-3

(for parameters, see Tables 1, 2, 3, 4, 5.)

“Cross” means that only two scans, rectangular to each other, were done; “surface” means that a 2D field was scanned.

As one can see, the centers of measurement do not necessarily have to coincide.

The monitored coordinates are not absolute. The measurements were made relative to a different coordinate system each time. NI 2007 was even made in another scanning sense (i.e. 180 degree rotated, or looking from the other side of the plane) as compared with NI 2005 and NI 2006. Apart from that, the scan resolution was different each time, varying from 0.15, 0.2, 0.3, 0.5, to 0.6 mm. Results were sometimes given in V, sometimes normalized to maximum or to center value. The measurements in the GI campaigns are rotated by 90 degrees, as compared to the NI campaigns, i.e. horizontal and vertical axes are swapped. On the other hand, channels *-3 are measured in both NI and GI, although using different wavelengths.

Therefore, the exact position of the flatfields within the detector area, or the exact position of the solar beam through the 3 mm precision hole, cannot be determined. In other words, it is not known whether the center of the scan (cross or surface) is identical to the center of the detector, or whether it is identical to the center of the solar beam. Nevertheless, the results of the “crosses” were compared with the “surfaces”, and the position of the flatfields relative to each other (i.e. their orientation on the detector plane) was confirmed.

Assuming

- a linear offset between NI 2005 and NI 2006 such that the center of the cross coincides, in average, with the center of the surface,
- rotation and offset between NI 2005 and GI 2005 such that the centers of the cross of channel 2-3 coincide,
- a linear offset between GI 2005 and GI 2006 such that the center of the cross coincides, in average, with the center of the surface,
- a linear offset between NI 2006 and NI 2007 such that the centers of the measurements coincide, in average, with each other,

then the locations of the various observations can be marked on the detector plane, in coordinates of NI 2006, as demonstrated in Figure 1 (following Tables 1,...,4 [black] and Table 5 [red]).

Table 1: **NI 2005 (crosses)**

ch.	wave.	hor.scan	at	vert.pos.	resol.	vert.scan	at	hor.pos.	resol.	/ mm
1-1	121nm	1.0, , 7.0	@	88.0	21*0.3	85.0, , 91.0	@	4.0	21*0.3	
1-2	210nm	1.0, , 7.0	@	101.0	21*0.3	98.0, , 104.0	@	4.0	21*0.3	
1-3	60nm	14.0, , 20.0	@	88.0	21*0.3	85.0, , 91.0	@	17.0	21*0.3	
2-1	121nm	1.0, , 7.0	@	149.0	21*0.3	146.0, , 152.0	@	4.0	21*0.3	
2-2	210nm	1.0, , 7.0	@	162.0	21*0.3	159.0, , 165.0	@	4.0	21*0.3	
2-3	60nm	12.5, , 21.5	@	149.0	31*0.3	146.0, , 152.0	@	17.0	21*0.3	
3-1	121nm	1.0, , 7.0	@	210.0	21*0.3	207.0, , 213.0	@	4.0	21*0.3	
3-2	210nm	1.0, , 7.0	@	223.0	21*0.3	220.0, , 226.0	@	4.0	21*0.3	
3-3	60nm	13.0, , 19.0	@	210.0	21*0.3	207.0, , 213.0	@	16.0	21*0.3	

Measured is “abs. signal (V), offset corrected”. The vertical position of the horizontal scan is not explicitly given; it is assumed to be in the middle of the vertical scan, and vice versa. (Channel 2-3 is indeed the only one to be scanned with 31 steps in horizontal direction.)

Table 2: **GI 2005 (crosses)**

ch.	wave.	hor.scan	at	vert.pos.	resol.	vert.scan	at	hor.pos.	resol.	/ mm
2-3	1nm	-10.00, . . . , -4.90	@	81.30	35*0.15	79.00, . . . , 83.50	@	-7.87	31*0.15	
2-3	18nm	-10.50, . . . , -5.40	@	81.31	35*0.15	79.00, . . . , 83.65	@	-8.09	32*0.15	
2-4	1nm	2.50, , 7.15	@	81.34	32*0.15	79.00, . . . , 83.65	@	4.86	32*0.15	
2-4	10nm	2.50, , 9.55	@	81.31	48*0.15	79.00, . . . , 84.10	@	4.86	35*0.15	
3-3	1nm	50.00, . . . , 55.60	@	81.34	29*0.2	79.00, . . . , 83.80	@	53.00	25*0.2	
3-3	18nm	51.00, . . . , 55.05	@	81.37	28*0.15	79.00, . . . , 84.55	@	52.94	38*0.15	
3-4	1nm	62.00, . . . , 68.20	@	81.23	32*0.2	79.00, . . . , 84.20	@	65.92	28*0.2	
3-4	10nm	63.50, . . . , 68.45	@	81.23	34*0.15	79.00, . . . , 83.95	@	65.65	34*0.15	

Measured is “Signal (V)”. The vertical position of the horizontal scan is explicitly given, and vice versa.

Table 3: NI 2006 (surfaces)

ch.	wave.	horizontal scan	resol.	vertical scan	resol.	/ mm
1-1	121.6nm	0.9, ..., 6.3	10*0.6	86.9, ..., 91.1	8*0.6	
1-2	210.0nm	0.9, ..., 5.7	9*0.6	99.1, ..., 103.9	9*0.6	
1-3	50.0nm	13.8, ..., 19.2	10*0.6	86.5, ..., 91.9	10*0.6	
2-1	121.6nm	0.2, ..., 4.2	9*0.5	148.4, ..., 152.4	9*0.5	
2-2	210.0nm	0.9, ..., 5.7	9*0.6	160.1, ..., 164.9	9*0.6	
2-3	50.0nm	13.6, ..., 19.0	10*0.6	147.6, ..., 153.0	10*0.6	
3-1	121.6nm	0.9, ..., 5.7	9*0.6	208.6, ..., 213.4	9*0.6	
3-2	210.0nm	0.9, ..., 5.7	9*0.6	221.0, ..., 225.8	9*0.6	
3-3	50.0nm	13.3, ..., 18.7	10*0.6	208.6, ..., 214.0	10*0.6	

Measured is the relative response, U(Diode)/I(Ring) with 3, 12, 24, 50, 100% aperture size, offset corrected, and normalized by the maximum signal. For comparison, the 100% values were used. The horizontal axis of channel 2-1 might be wrong by 0.7 mm.

Table 4: GI 2006 (surfaces)

ch.	wave.	horizontal scan	resol.	vertical scan	resol.	/ mm
1-3	18nm	-70.14, ..., -66.54	13*0.3	79.43, ..., 83.03	13*0.3	
1-4	10nm	-57.31, ..., -53.71	13*0.3	79.41, ..., 83.01	13*0.3	
2-3	18nm	-9.00, ..., -5.40	13*0.3	79.45, ..., 83.05	13*0.3	
2-4	10nm	3.65, ..., 7.25	13*0.3	79.43, ..., 83.03	13*0.3	
3-3	18nm	51.80, ..., 55.40	13*0.3	79.50, ..., 83.10	13*0.3	
3-4	10nm	64.55, ..., 68.15	13*0.3	79.28, ..., 82.88	13*0.3	

Measured is the relative responsivity, normalized to the value of the center point. The coordinates of the center points are given [this was not considered in the previous version of this report]. They are only slightly offset from GI 2005.

Table 5: NI 2007 (surfaces)

ch.	wave.	horizontal scan	resol.	vertical scan	resol.	/ mm
1-1	121.6nm	15.0, ..., 21.6	12*0.6	76.0, ..., 80.8	9*0.6	
1-2	210.0nm	15.2, ..., 21.8	12*0.6	88.6, ..., 93.4	9*0.6	
1-3	50.0nm	1.8, ..., 8.4	12*0.6	75.9, ..., 80.7	9*0.6	
2-1	121.6nm	14.9, ..., 21.5	12*0.6	136.7, ..., 141.5	9*0.6	
2-2	210.0nm	15.1, ..., 21.7	12*0.6	149.7, ..., 154.5	9*0.6	
2-3	50.0nm	2.0, ..., 8.6	12*0.6	136.8, ..., 141.6	9*0.6	
2-3	50.0nm	2.0, ..., 8.6	12*0.6	136.8, ..., 141.6	17*0.3	
3-1	121.6nm	15.0, ..., 21.0	11*0.6	198.0, ..., 202.8	9*0.6	
3-2	210.0nm	15.0, ..., 21.6	12*0.6	210.6, ..., 215.4	9*0.6	
3-3	50.0nm	1.7, ..., 8.3	12*0.6	197.8, ..., 202.6	9*0.6	

Measured is the relative responsivity, normalized to the maximum signal. The horizontal scanning sense had to be reversed to make the measurements comparable to the other campaigns.

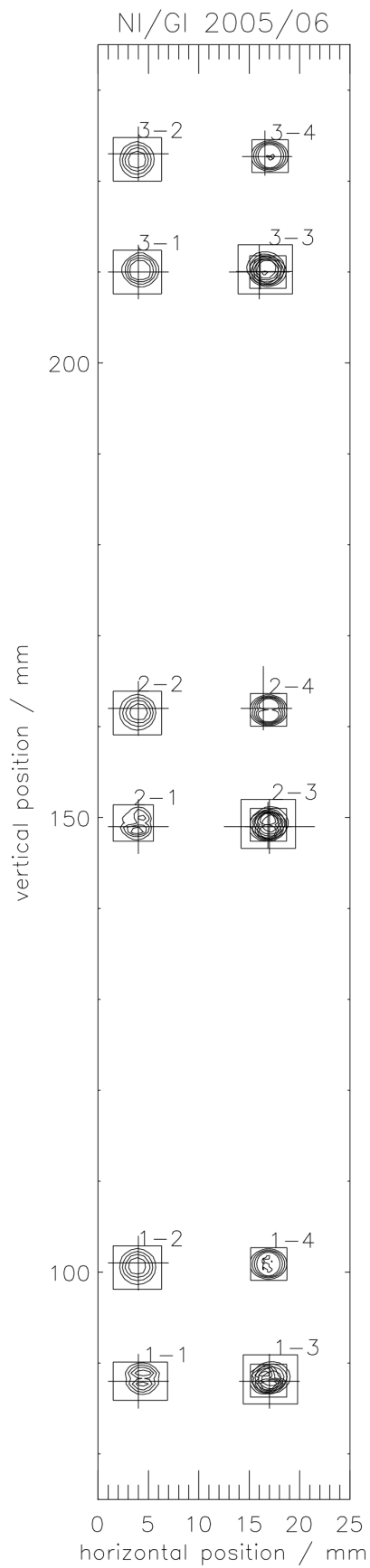
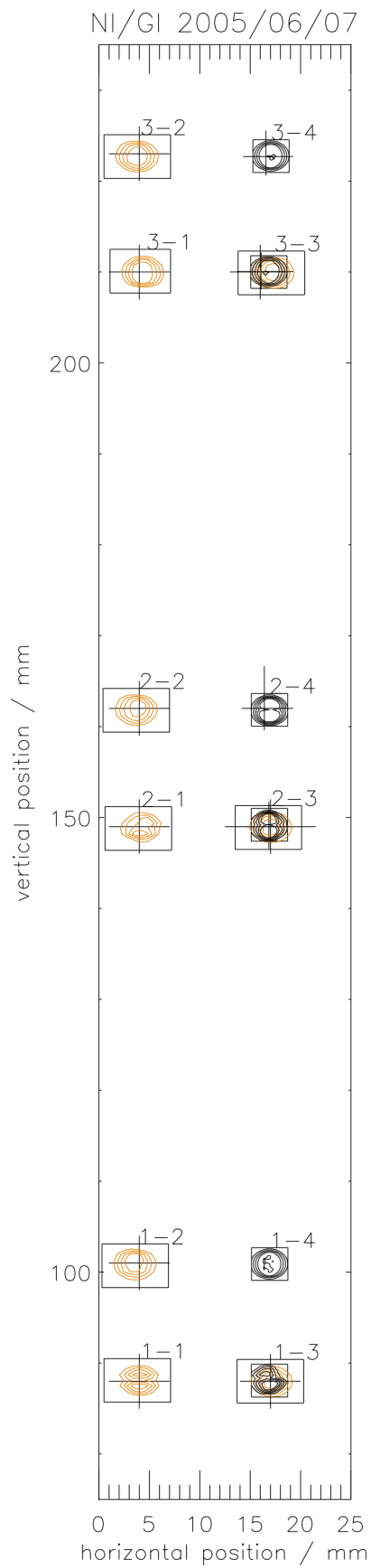


Figure 1.



The flatfield measurements have an influence on the responsivity and thus – indirectly – on the radiometric model. During the BESSY campaigns, responsivity could not be measured under realistic in-flight conditions. Rather, it was only measured at selected wavelengths, and it was not measured such that the beam covered most of the detector surface, as the Sun eventually will: 7.068 square millimeter, i.e. the area of the 3-mm-diameter precision aperture. During the most recent responsivity tests, the NI beam for measuring channels *-1, *-2, and *-3 was a rectangle of 2.5 mm (horizontal) x 1.0 mm (vertical). The GI beam for measuring channels *-3, and *-4 was a square of 1.5 mm x 1.5 mm.

Usually, the detectors are more sensitive in the center. Nevertheless, until now the responsivity measurements were treated as if the response was homogeneous all over the detector. Therefore, the effect of inhomogeneity had to be simulated with the help of their flatfields. In most cases, the simulation result was such that the responsivity had been overestimated by a factor > 1.

In detail, the simulations lead to the following factors:

channel	NI2006	GI2006	NI2007	selected
1-1 MSM	1.05		0.96	1.01
1-2 PIN	1.18		1.15	1.16
1-3 MSM	1.25	1.32	1.24	1.28
1-4 AXUV		1.19		1.19
2-1 MSM	0.93		1.12	1.03
2-2 PIN	1.19		1.16	1.18
2-3 MSM	1.22	1.24	1.19	1.22
2-4 MSM		1.18		1.18
3-1 AXUV	1.16		1.10	1.13
3-2 PIN	1.20		1.16	1.18
3-3 AXUV	1.19	1.22	1.17	1.20
3-4 AXUV		1.19		1.19

Therefore, the responsivity curves in the nominal wavelength intervals will be *divided* by this factor (see Section IV, p. 20).

The NI rasters were usually taken with 0.6 mm step size, the GI rasters with 0.3 mm. For channel 2-3, two rasters were made at NI 2007; one of them with 0.6 mm vertical step size, the other with 0.3 mm. The simulation results both deliver a factor 1.19, so this does not point to an influence of raster resolution. Since there is no reason to trust the results from NI 2007 more than those of NI 2006, the factors were averaged. Thus, the two contradictory results for MSM channels 1-1 and 2-1, who both have a complicated topology, do not lead to a major correction. In the case of channels *-3, the NI results (taken at 50 nm wavelength) are averaged with the GI result (taken at 18 nm). As one can see, apart from channels 1-1 and 2-1, the results are rather consistent, especially within the group of PIN and AXUV detectors.

On the next three pages, Figures 2-1, 2-2, and 2-3 demonstrate the simulations for the three LYRA heads.

For the detectors of the Aluminium channels *-3, the GI campaign values were used for Figures 2 and 3, since the short-wavelength part probably dominates the output signal of these channels.

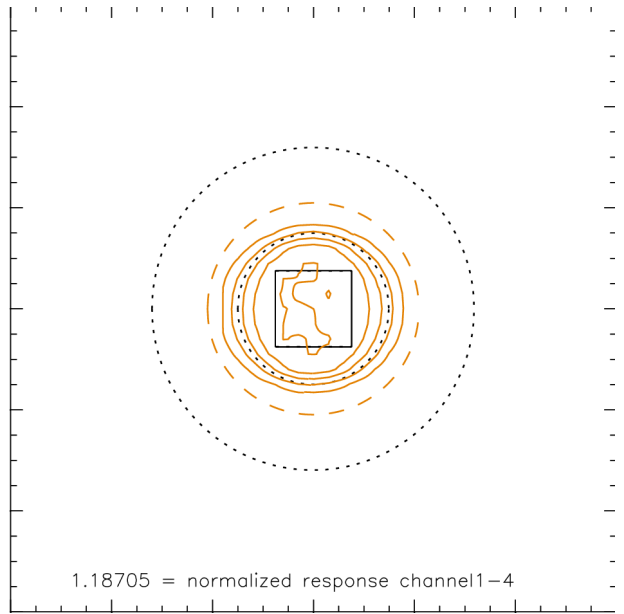
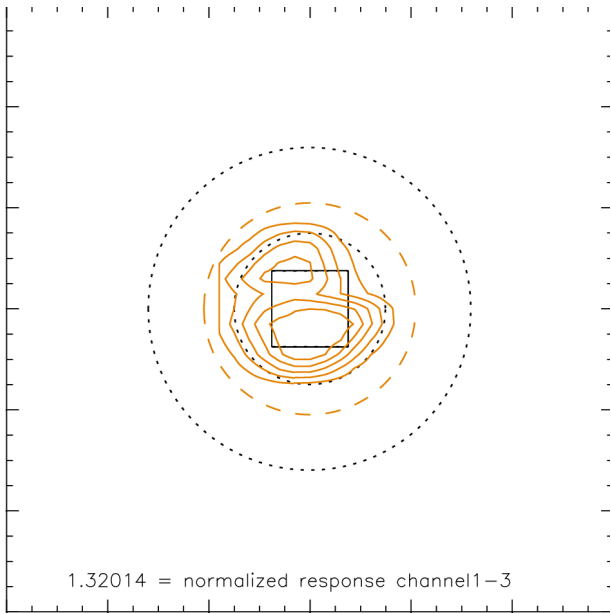
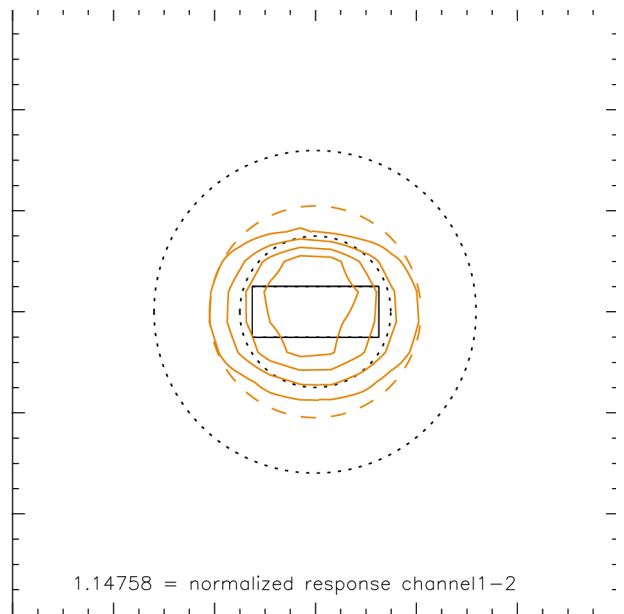
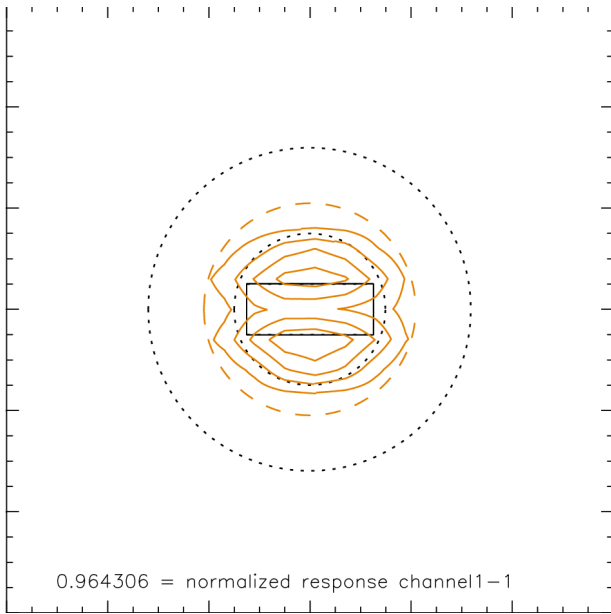


Figure 2-1.

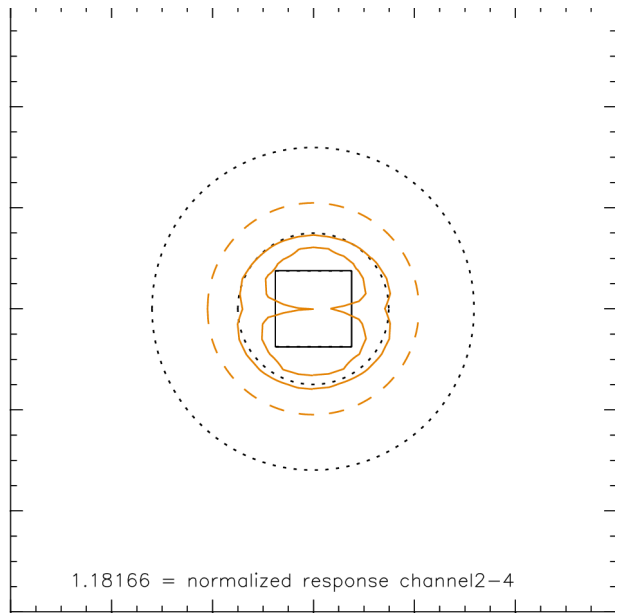
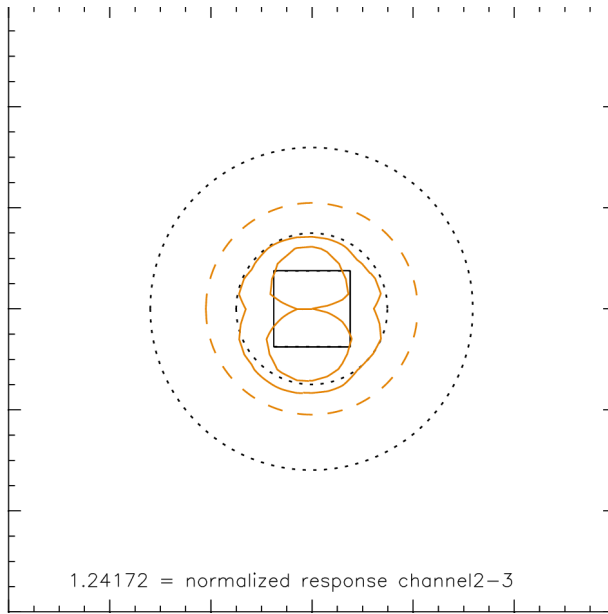
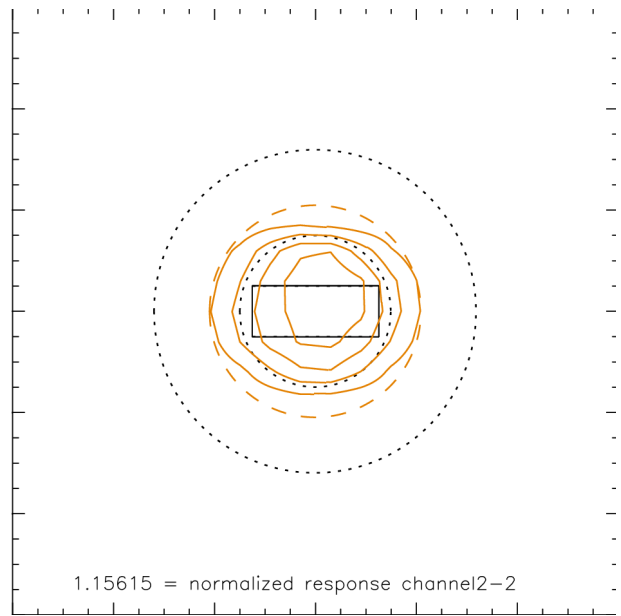
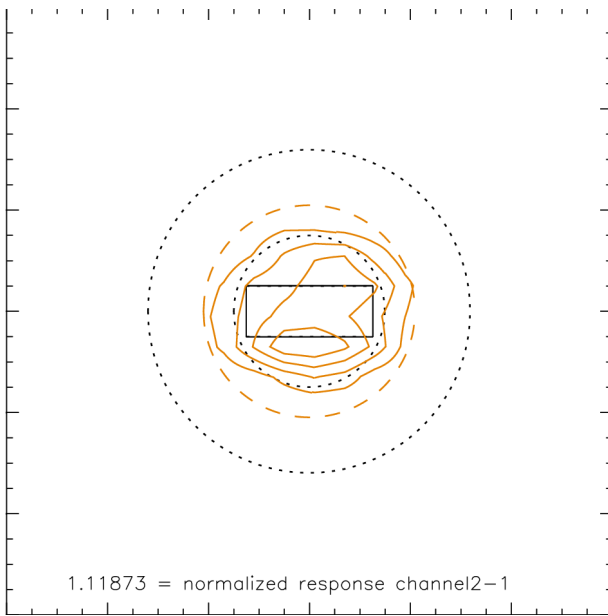


Figure 2-2.

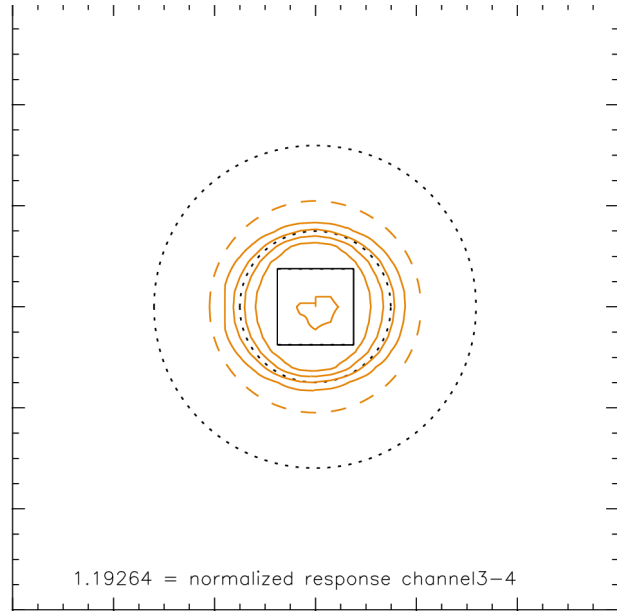
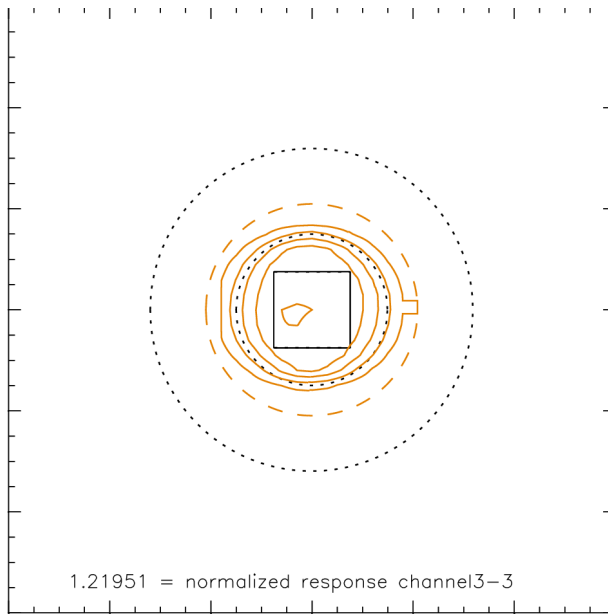
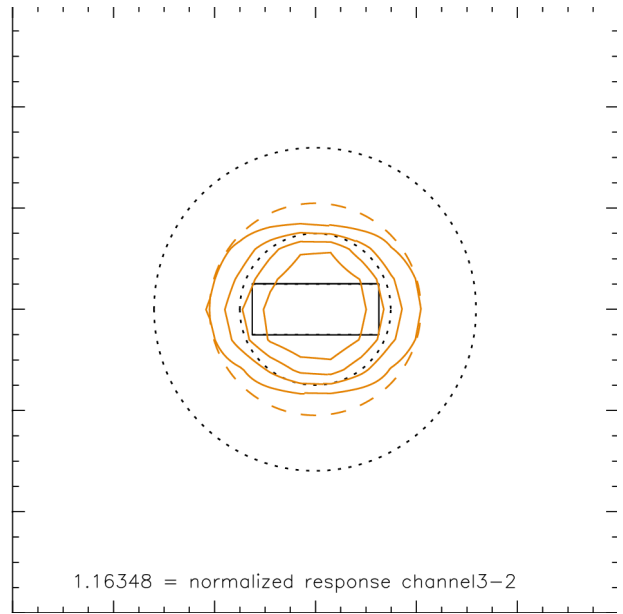
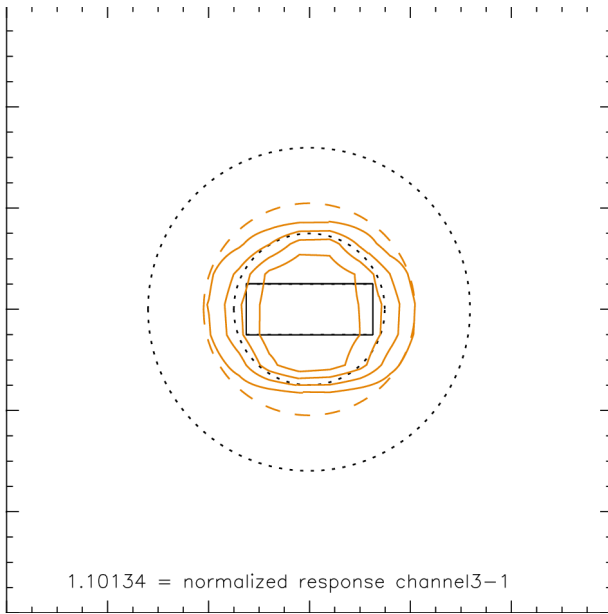


Figure 2-3.

Based on this common orientation, reactions to off-pointing can be simulated in a way described in another report (cf. *IED_20061025_LYRA_Calibration.pdf*). Additionally, off-pointing has been simulated here covering a whole range of possible values, namely from -1 degree to +1 degree, in east-west as well as in north-south direction. This grid of simulations leads to a surface of normalized responses as shown on the next three pages in Figures 3-1, 3-2, and 3-3. It is assumed that north is up (i.e. on the upper side of the detector plane as shown in the previous Figures 1 and 2), and that the solar beam hits the detector plane in the same sense as one looks onto the figures. A possible roll angle should be implemented in the simulation software (TBD). - Numbers within the images show the variations in the correction factor (maximum and minimum for +/- 1 degree off-pointing, and for +/- 5 arcmin off-pointing around the center position).

It is not claimed here that the in-flight reaction of LYRA will be exactly like the simulations. The real positions of the various detectors on the plane might be slightly different, the nominal pointing might not be exactly centered, the response to the real solar beam might differ from the BESSY test situation in many ways (small beam size, fixed wavelength). Nevertheless, the simulation technique presented here may help to interpret in-flight findings during the commissioning phase.

It is suggested to test various off-pointing positions during the commissioning phase in co-operation with SWAP, in order to get – for each LYRA channel - a grid of relative responses comparable to the simulations described here. In the most favourite case, the simulated grids can be confirmed, maybe with a linear offset. Combining the simulations and the in-flight tests, there should emerge a tabled function of relative responses - for each channel - with pointing coordinates and roll angle as input, and a correction factor around 1.0 (= nominal pointing) as output.

Simulations show that +/- 1 degree off-pointing leads to approx. 20-25% reduction from the nominal response. Off-pointing in the order of the nominal jitter of PROBA2 (5 arcmin, TBC) leads to fluctuations of approx. +/- 1% around the nominal response. Off-pointing in the order of the promised maximal offset between SWAP and LYRA (2 or 10 or 20 arcsec over 10 or 60 s, TBC) will therefore not be detectable.

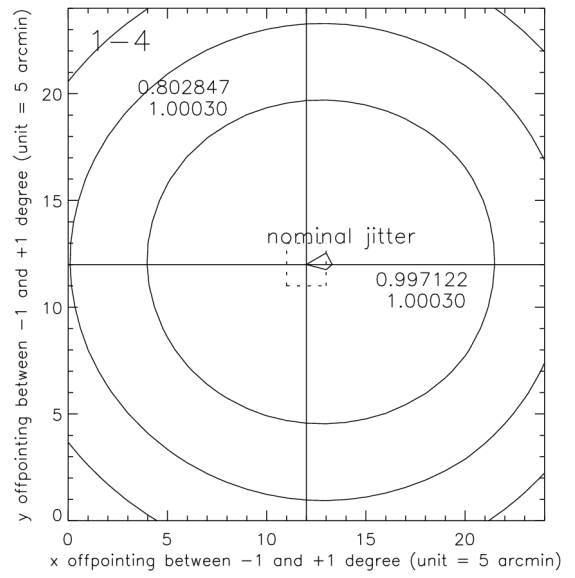
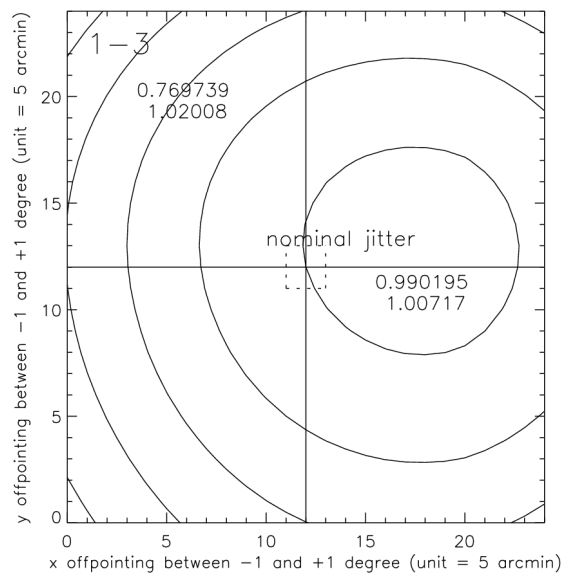
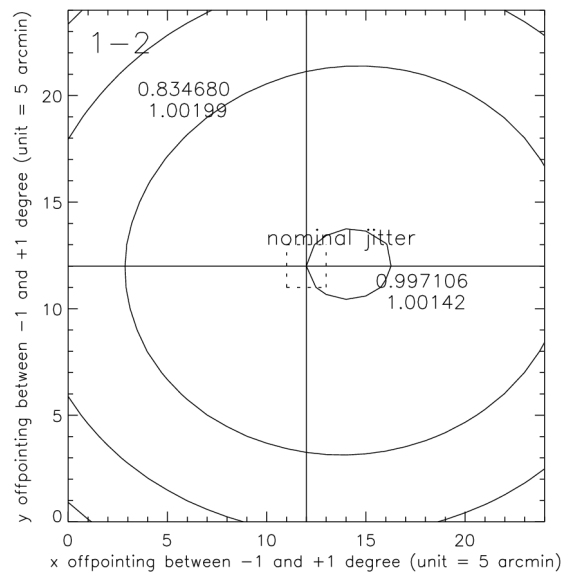
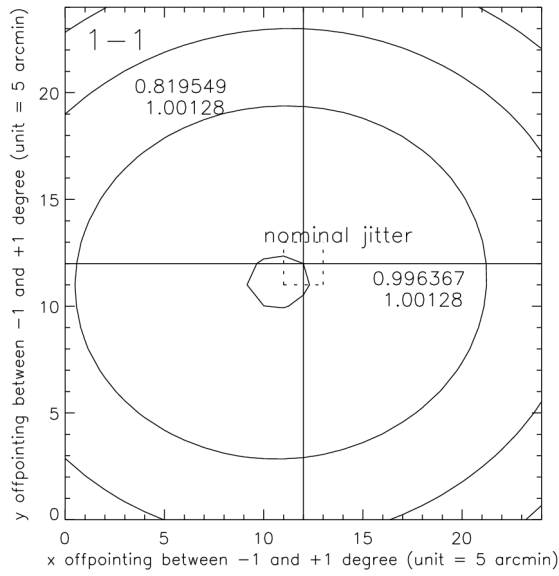


Figure 3-1.

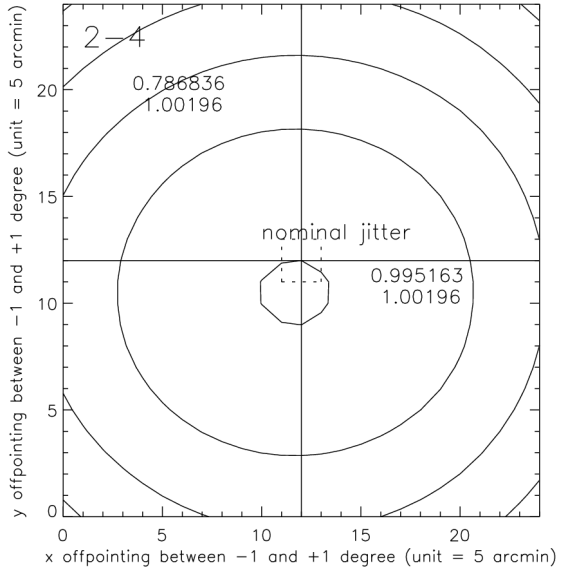
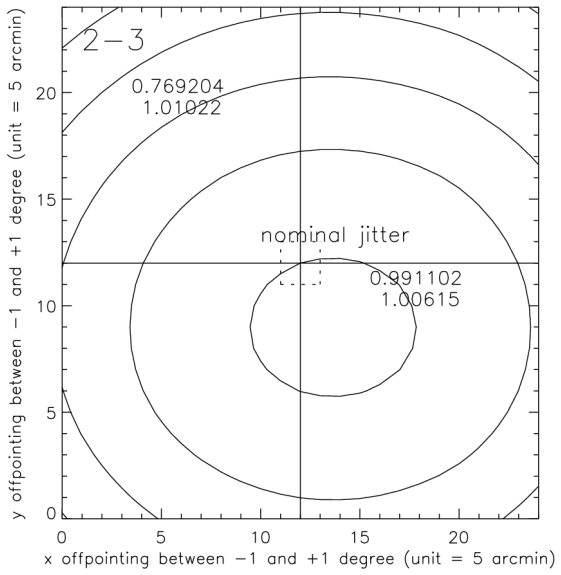
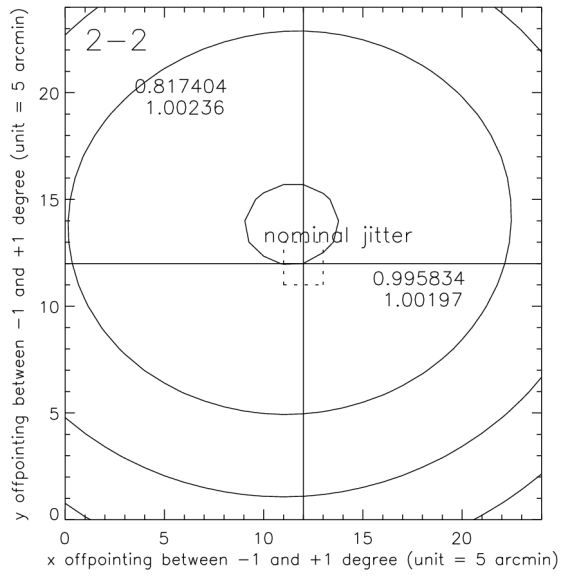
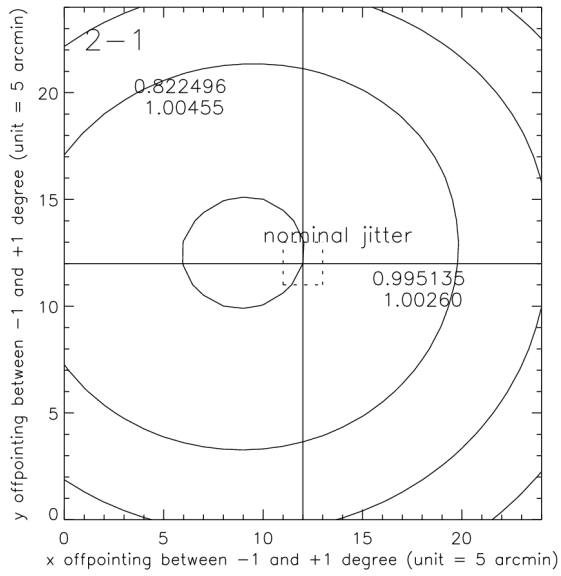


Figure 3-2.

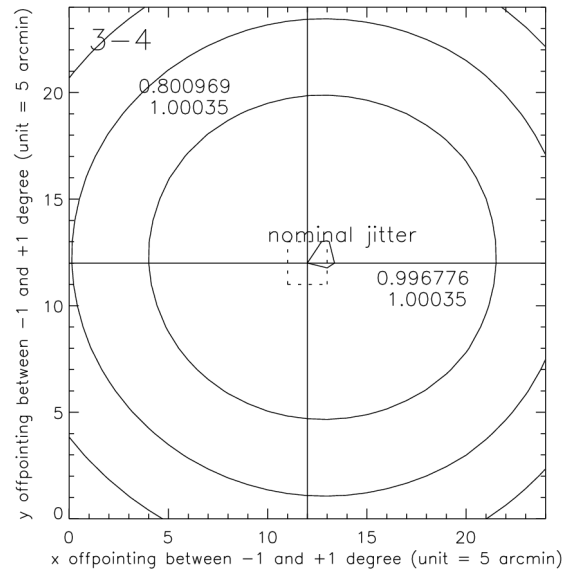
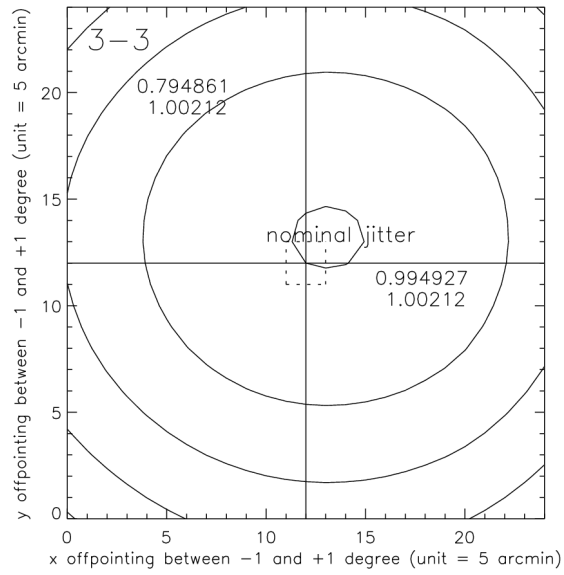
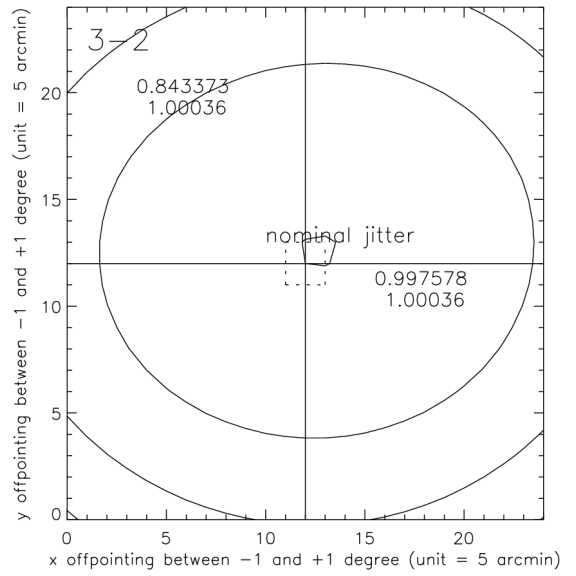
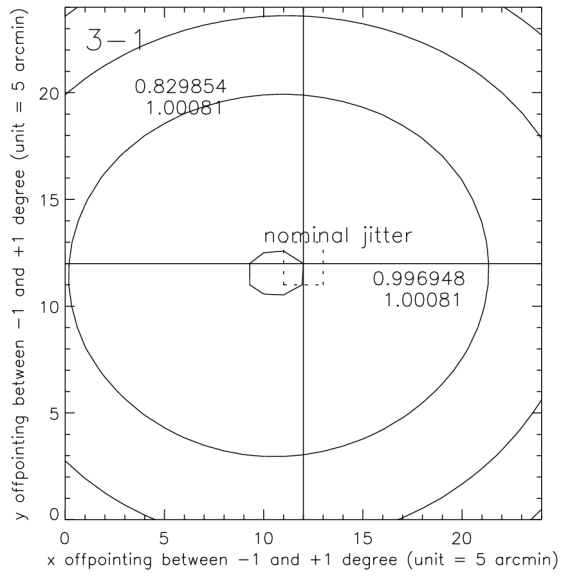


Figure 3-3.

III. Simulations with Davos Solar Spectrum

During tests of the LYRA instrument at PMOD/WRC in Davos on 07 Apr 2006, the channels were exposed to sunlight on ground (heliostat, sunny conditions, clear sky), and the solar spectrum was recorded together with the channels' reaction over time.

The solar spectrum is shown in the following simulation (example: Channel 1-1, see figure next page). The reaction of LYRA over time is available in the file *Davos_Sun_070406.xls*.

In the simulations, the various combined filter transmittances and detector responsivities were multiplied with the solar spectrum, in order to integrate the response of the radiometric model. These results can then be compared to the values observed in Davos, see table below. - It has to be noted that responsivities in the near-UV, visible, and infrared range were calculated on theoretical considerations, and the measured responsivities around the nominal bandwidths were thus extended in the longer-wavelength direction. The exact values around the nominal bandwidths, on the other hand, are irrelevant for these simulations, since the Davos solar spectrum is always outside their range.

channel		new simulation		old simul.	observed	err
-----		-----		-----	-----	---
1-1 Ly XN	+ MSM12	(2.51684e-13 A)	251.684 fA	251.519 fA	0.2 pA	OK
1-2 Herzberg	+ PIN10	(5.97465e-14 A)	59.7465 fA	59.672 fA	0.0 pA	OK
1-3 Aluminium	+ MSM11	(4.31285e-19 A)	431.285 zA	455.338 zA	0.0 pA	OK
1-4 Zr (300nm)	+ AXUV20D	(1.36846e-13 A)	136.846 fA	136.829 fA	1.25 pA	*10
2-1 Ly XN	+ MSM21	(9.75385e-13 A)	975.385 fA	974.180 fA	0.4-0.45 pA	/2
2-2 Herzberg	+ PIN11	(7.29704e-14 A)	72.9704 fA	72.958 fA	0.0-0.5 pA	OK
2-3 Aluminium	+ MSM15	(2.05091e-19 A)	205.091 zA	226.566 zA	0.0 pA	OK
2-4 Zr (150nm)	+ MSM19	(8.11899e-15 A)	8.1190 fA	8.118 fA	0.0-0.02 pA	OK
3-1 Ly N+XN	+ AXUV20A	(3.58272e-11 A)	35.8272 pA	35.834 pA	82 - 88 pA	*2.5
3-2 Herzberg	+ PIN12	(5.95234e-14 A)	59.5234 fA	59.532 fA	0.0 pA	OK
3-3 Aluminium	+ AXUV20B	(2.97916e-12 A)	2.9792 pA	3.000 pA	7.0-8.0 pA	*2.5
3-4 Zr (300nm)	+ AXUV20C	(1.36846e-13 A)	136.846 fA	136.829 fA	2.5-2.9 pA	*20

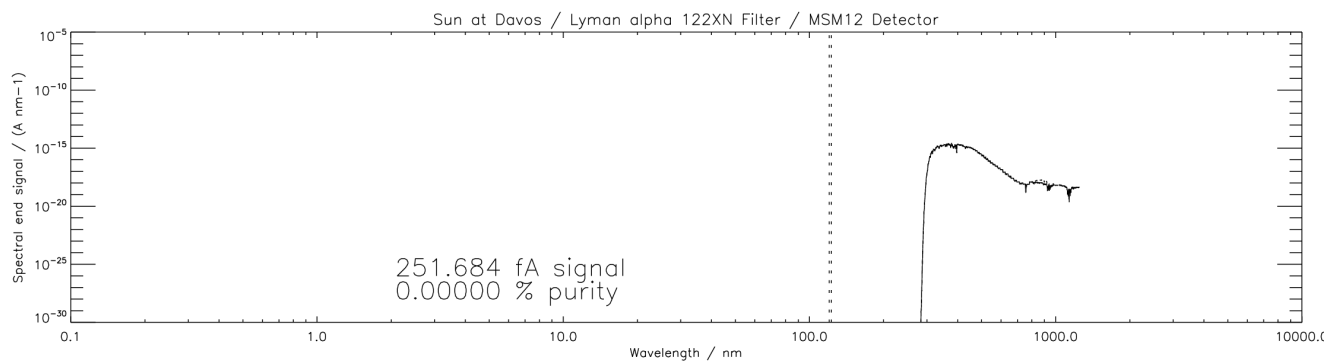
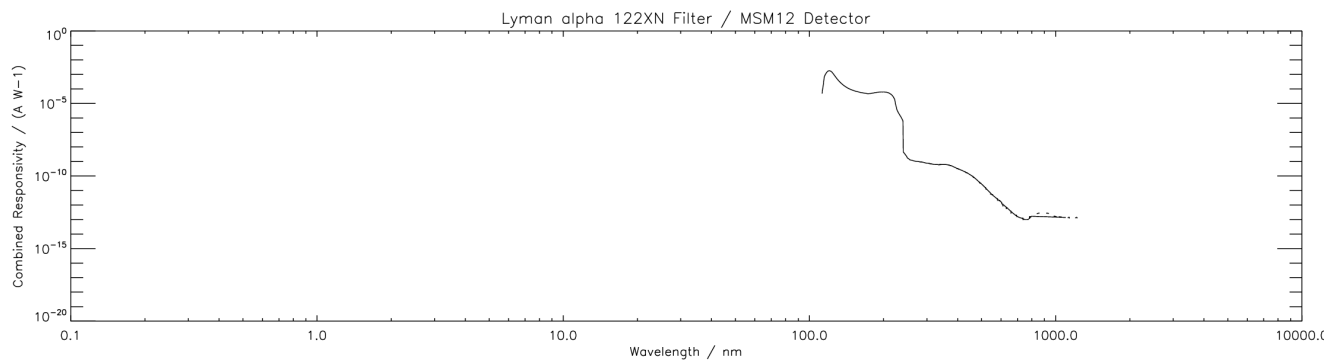
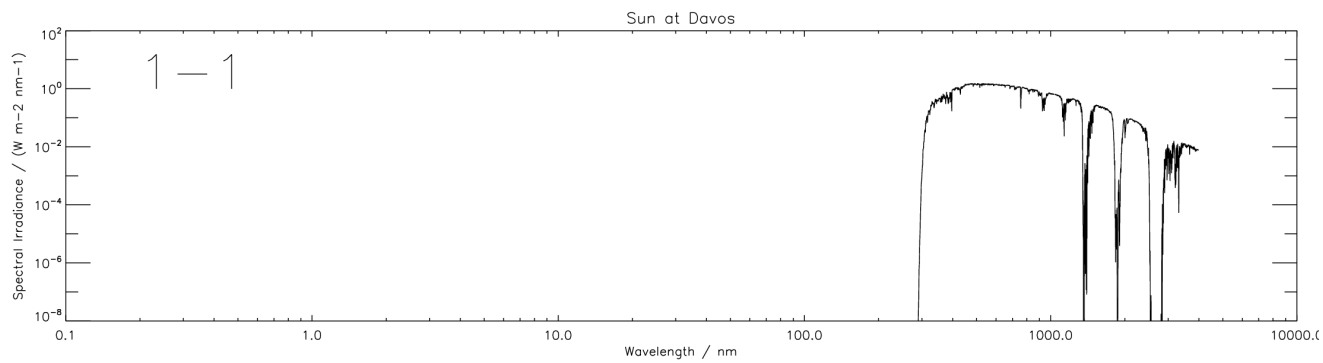
The “old” simulations were independently done for the radiometric model as presented on the LYRA web pages. The values are close enough to assume that the same numbers and methods were used.

The PIN detectors behave such that practically no output was expected and no output was observed (thus “OK”).

The MSM detectors either have no significant output observed where none was expected, or output was observed within the expected range (thus “OK”). The only exception is channel 2-1, where the observed output is only half the expected value.

The AXUV detectors all have higher outputs than was expected, from factor 2.5 to 20. If one considers the values to be expected from the Sun while in space, the ~pA changes in channels 1-4, 3-3, and 3-4 will probably only have negligible influences. For channel 3-1, the expected purity will fall from 80% to something like 45%, but this was already anticipated and discussed in several meetings. The problem remaining is the possibility of a pinhole in channels 3-1 and 3-3, which has to be watched carefully, since an increasing size may reduce the signal purity. - The dark current values in the Davos data file are always 0 pA, so a temperature influence can be excluded.

Resulting modifications for the long-wavelength part of the responsivities are suggested in Section IV.



IV. Suggested Responsivity Changes

It follows from Section II that most of the responsivities around the nominal bandwidth were overestimated and therefore have to be reduced. From the simulations in Section III, it follows that some of the responsivities in the long-wavelength range (near UV, visible, and infrared) were underestimated, one was overestimated. As a result, it is suggested here that the responsivity curves, as constructed in Section I, shall be modified (divided or multiplied) as follows:

channel		nominal range modification	long wavelength modification
-----		-----	-----
1-1 Ly XN	+ MSM12	-	-
1-2 Herzberg	+ PIN10	/1.16	-
1-3 Aluminium	+ MSM11	/1.28	-
1-4 Zr (300nm)	+ AXUV20D	/1.19	*10
2-1 Ly XN	+ MSM21	-	/2
2-2 Herzberg	+ PIN11	/1.18	-
2-3 Aluminium	+ MSM15	/1.22	-
2-4 Zr (150nm)	+ MSM19	/1.18	-
3-1 Ly N+XN	+ AXUV20A	/1.13	*2.5
3-2 Herzberg	+ PIN12	/1.18	-
3-3 Aluminium	+ AXUV20B	/1.20	*2.5
3-4 Zr (300nm)	+ AXUV20C	/1.19	*20

On the following three pages, the new curves are shown on a log-log scale. Nominal spectral intervals of the channels are marked in red.

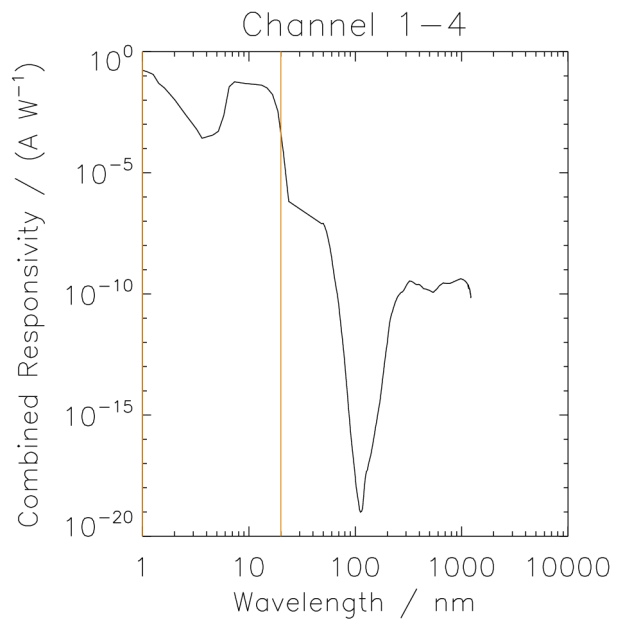
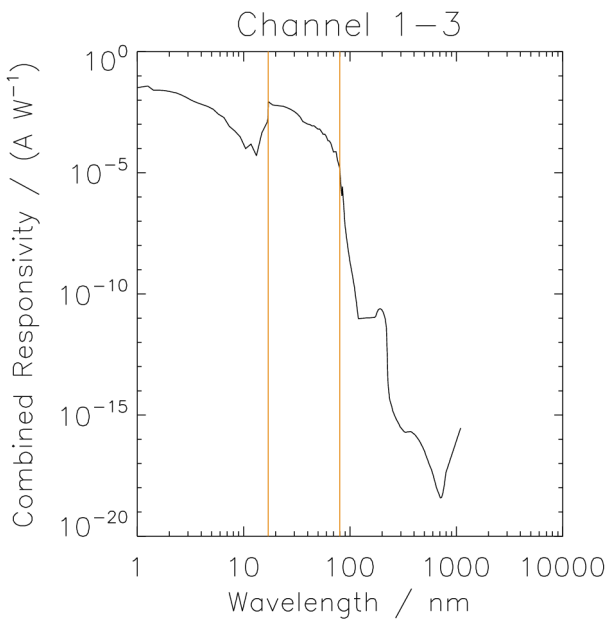
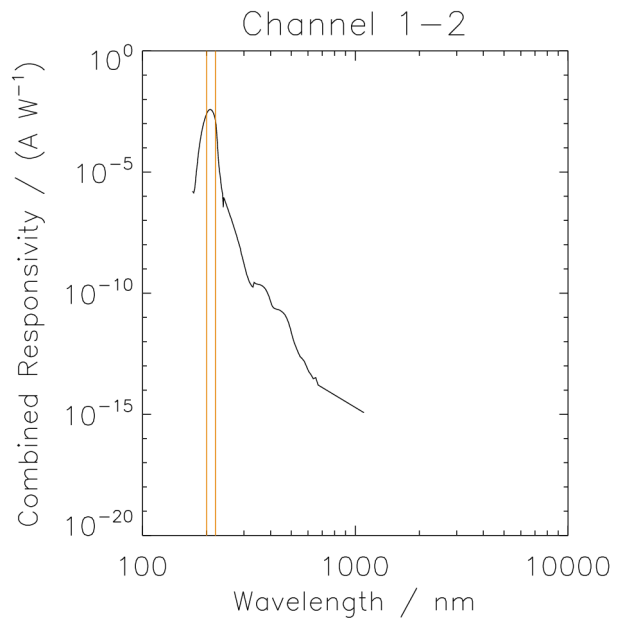
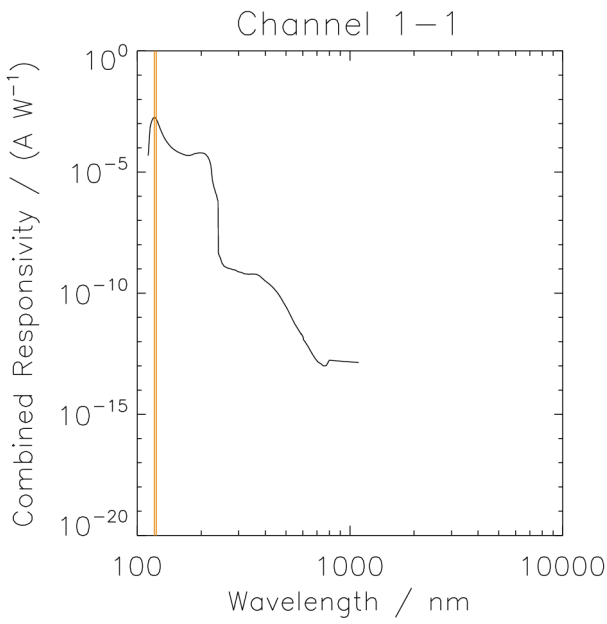
As an Appendix, the contents of one file (example: Channel 1-1) are shown to demonstrate the format.

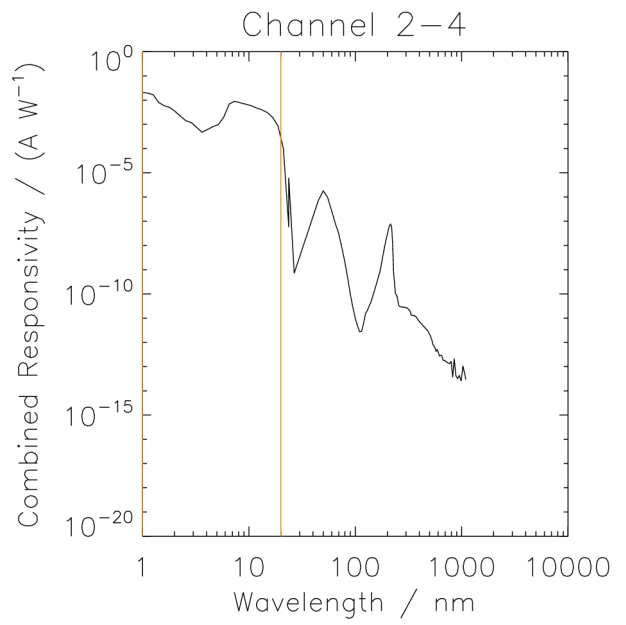
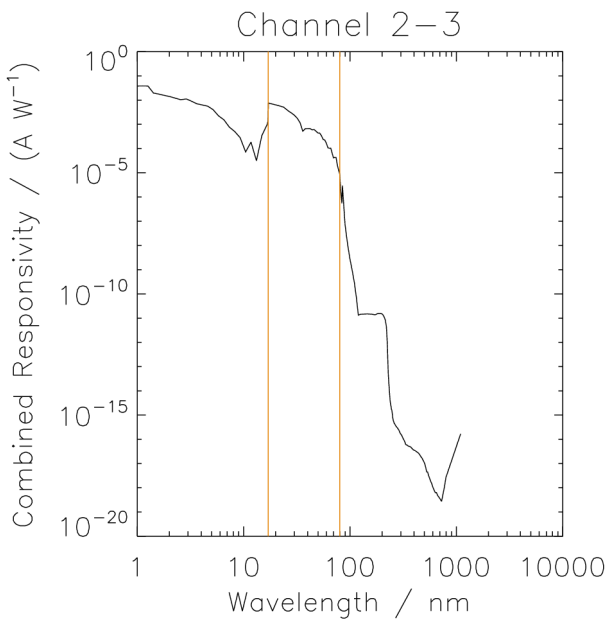
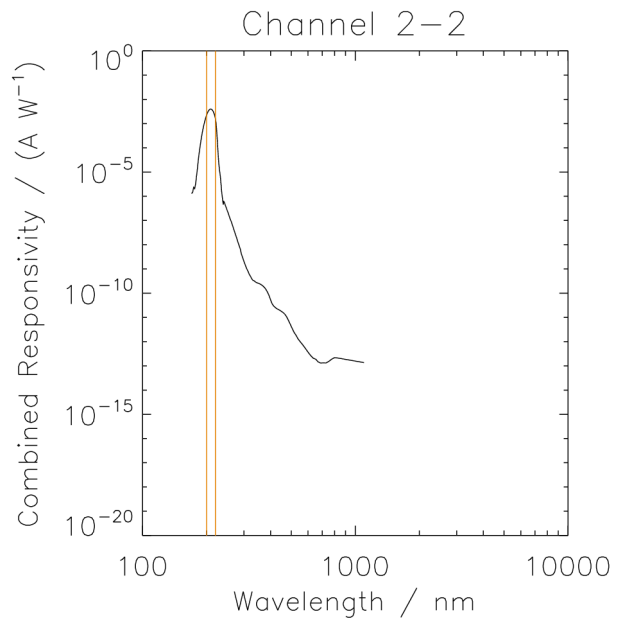
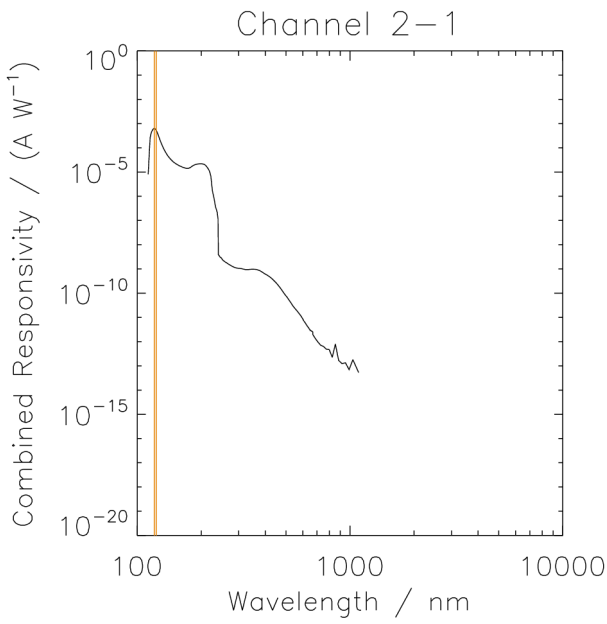
All responsivity curves are available in ASCII text format from the website

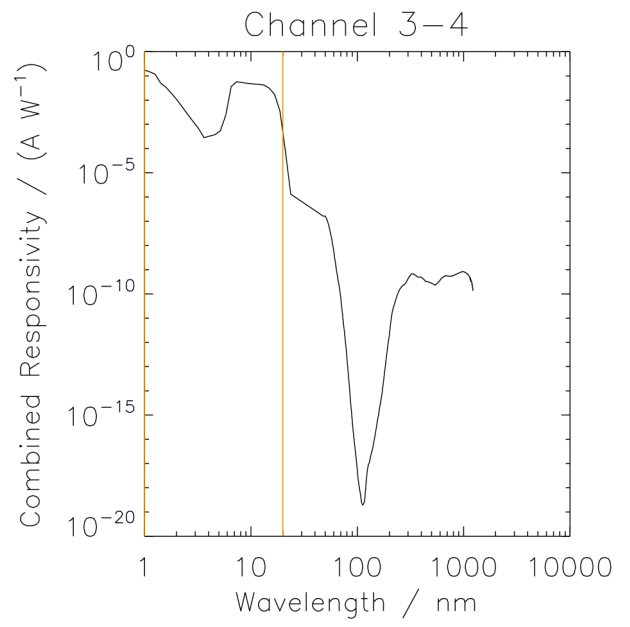
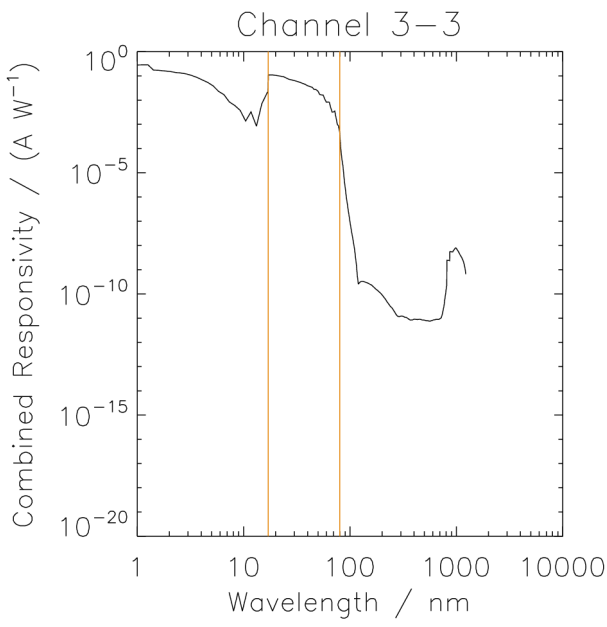
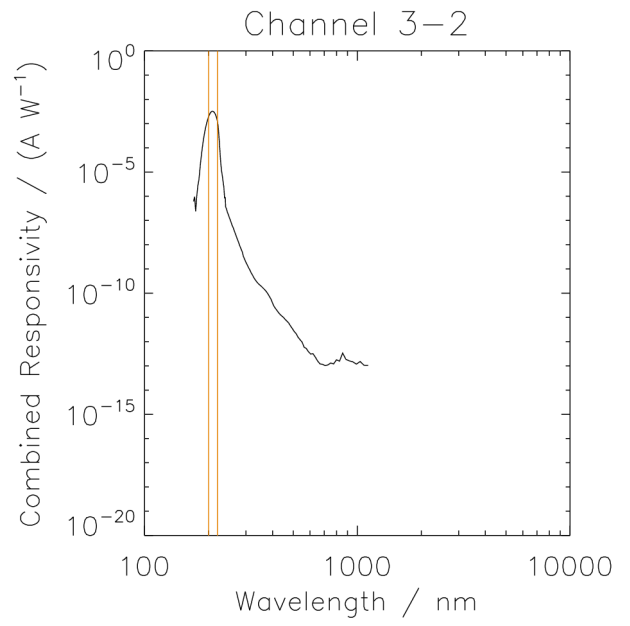
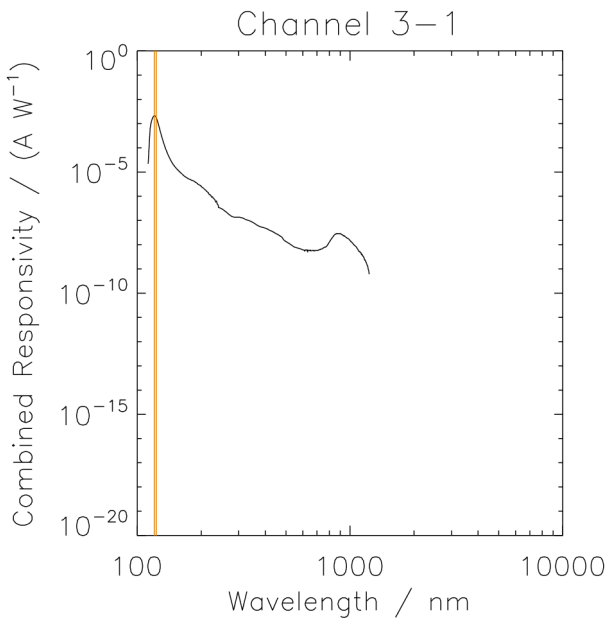
<http://solwww.oma.be/users/dammasch/reports.html>

under "Data Files". The files are called *resp_ch**.dat*. They contain four header lines and a number of data lines (given as *extended list length*). These also include the responsivities of the long-wavelength extension. The first lines (number given as *list length*) are the responsivities around the nominal-range interval, as measured in the most recent BESSY campaign.

Error bars and uncertainties are not given here, but they are available, at least for the nominal wavelength intervals. In the future – after the re-calculation of the LYRA radiometric model - they will be used to calculate a measure for the reliability of the pre-flight calibration (TBD).







Appendix

LYRA Channel 1-1 (Ly XN + MSM12) Combined Responsivity, 16 Jan 2008

77 = list length

154 = extended list length

lambda / nm	resp / (A/W)
112.500	4.82656e-05
115.000	0.000718533
116.000	0.00100099
117.000	0.00125867
117.500	0.00139742
118.000	0.00150644
118.500	0.00161546
119.000	0.00169475
119.500	0.00174430
120.000	0.00179386
120.500	0.00178394
121.000	0.00176412
121.600	0.00170466
122.000	0.00167493
122.500	0.00159564
123.000	0.00151635
123.500	0.00141724
124.000	0.00130823
125.000	0.00110010
126.000	0.000913776
128.000	0.000634291
130.000	0.000455897
132.000	0.000336967
134.000	0.000260654
136.000	0.000209118
138.000	0.000172448
140.000	0.000145689
142.000	0.000124876
144.000	0.000109019
146.000	9.78196e-05
148.000	8.84044e-05
150.000	8.08721e-05
152.000	7.49257e-05
154.000	6.97720e-05
156.000	6.58077e-05
158.000	6.22398e-05
160.000	5.92666e-05
162.000	5.65907e-05
164.000	5.41130e-05
166.000	5.23290e-05
168.000	5.04460e-05
170.000	4.88603e-05
172.000	4.75719e-05
174.000	4.72745e-05
176.000	4.79683e-05
178.000	4.90585e-05
180.000	5.09415e-05
182.000	5.24281e-05
184.000	5.46085e-05
186.000	5.66898e-05

188.000	5.81764e-05
190.000	5.93657e-05
192.000	6.01586e-05
194.000	6.08523e-05
196.000	6.18434e-05
198.000	6.13479e-05
200.000	6.14470e-05
202.000	6.11497e-05
204.000	6.00595e-05
206.000	5.88702e-05
208.000	5.63925e-05
210.000	5.31219e-05
212.000	4.83647e-05
214.000	4.36075e-05
216.000	3.82557e-05
218.000	3.22101e-05
220.000	2.55699e-05
222.000	1.91278e-05
224.000	8.79088e-06
226.000	4.32111e-06
228.000	2.98315e-06
230.000	2.27948e-06
232.000	1.73439e-06
234.000	1.37760e-06
236.000	1.08028e-06
238.000	8.08721e-07
240.000	6.27354e-07
240.780	4.45070e-09
243.140	3.60027e-09
245.540	2.92386e-09
248.000	2.29947e-09
250.510	1.69358e-09
253.060	1.54080e-09
255.670	1.31603e-09
258.330	1.22986e-09
261.050	1.18420e-09
263.830	1.13637e-09
266.670	1.07776e-09
269.570	1.04689e-09
272.530	1.02043e-09
275.560	9.95444e-10
278.650	9.61582e-10
281.820	9.39951e-10
285.060	9.27102e-10
288.370	8.94492e-10
291.760	8.57839e-10
295.240	7.99445e-10
298.800	7.66473e-10
302.440	7.42311e-10
306.170	7.25990e-10
310.000	6.98660e-10
313.920	6.70211e-10
317.950	6.42630e-10
322.080	6.19836e-10
326.320	6.12612e-10
330.670	6.10315e-10
335.140	5.93491e-10

339.730	6.09208e-10
344.440	6.12172e-10
349.300	6.12499e-10
354.290	6.10580e-10
359.420	6.00995e-10
364.710	5.86972e-10
370.150	5.53376e-10
375.760	5.19536e-10
381.540	4.61447e-10
387.500	4.08902e-10
393.650	3.60690e-10
400.000	3.17435e-10
406.560	2.86632e-10
413.330	2.54916e-10
420.340	2.25541e-10
427.590	1.96454e-10
435.090	1.68968e-10
442.860	1.41956e-10
450.910	1.17761e-10
459.260	9.61999e-11
467.920	7.52260e-11
476.920	5.75909e-11
486.270	4.25639e-11
496.000	3.17725e-11
506.120	2.34182e-11
516.670	1.63761e-11
527.660	1.13468e-11
539.130	7.72527e-12
551.110	5.31928e-12
563.640	3.86587e-12
576.740	2.79257e-12
590.480	1.98399e-12
590.480	2.15527e-12
604.880	1.43955e-12
604.880	1.20183e-12
620.000	9.04051e-13
620.000	8.84978e-13
635.900	6.31135e-13
652.630	4.15654e-13
670.270	2.77574e-13
688.890	1.93153e-13
708.570	1.42637e-13
729.410	1.22085e-13
751.520	9.82039e-14
775.000	1.00604e-13
800.000	1.68223e-13
1100.00	1.35714e-13